Pergamon

Int. J. Heat Mass Transfer. Vol. 38, No. 9, pp. 1587–1596, 1995

0017-9310/95 $9.50+0.00

0017-9310(94)00290-8

Air filtration with moisture and frosting phase changes in fiberglass insulation—I. Experiment

D. R. MITCHELL, Y.-X. TAO† and R. W. BESANT

Department of Mechanical Engineering, University of Saskatchewan, Saskatoon, Saskatchewan, Canada S7N 0W0

(*Received* 7 *February* 1994 *and in final form* 18 *August* 1994)

Abstract—A laboratory apparatus has been constructed to subject fiberglass insulation to one-dimensional moist airflow and heat transfer with temperatures from 20 to −20°C. Using this apparatus, the effects of air exfiltration and infiltration on the heat and moisture transport characteristics within a medium density fiberglass insulation material are investigated experimentally for one-dimensional transient conditions. The experimental results, which are typical of cold climate building envelope applications, indicated that the adsorption process had a significant influence on the temperature distribution over much of the warm portion of the slab during air exfiltration shortly after the tests began. Furthermore, for all of the air exfiltration tests carried out, the majority of the moisture and frost accumulation was within the insulation slab adjacent to the cold surface. For air infiltration, it was discovered that the drying rate was substantially higher for lower airflow rates.

1. INTRODUCTION

In the past decade or two, thick layers of fiberglass insulation have been used to conserve energy within building and refrigerated space envelopes. Failure to eliminate the natural convection of air and moisture diffusion within typical fiberglass insulated roof structures in a cold climate has been shown to reduce the apparent thermal resistance of the insulation by up to a factor of two [1]. The accumulation of moisture not only increases the energy transfer across the insulation, it can also lead to mold growth, degradation of any organic materials such as wood, rust damage to any metallic components, freezing damage in the condensation zone at low temperatures, as well as an overall reduction in the quality of the insulation [2]. To inhibit the flow of air and moisture through the wall structure a vapor retarder is a required building construction detail in cold climates [3], especially where the insulation systems operate below freezing conditions [4]. However, in practice, the consequences of the frequently observed failure of the vapor retarder in air-tight structures due to installation problems (among other factors) are well known in the design and consulting communities [5].

Moisture transport within building wall and ceiling insulation generally takes place either through the process of vapor diffusion, or as a result of the flow of moist air through the insulation. The flow of moist air through such building envelopes is a consequence of pressure differences across the permeable envelope materials caused by wind pressure effects, different temperature gradients inside and outside, or the air circulation fans used within buildings.

The main processes involved with the accumulation of moisture within the insulation are either adsorption or condensation/frosting. Adsorption involves the collection of water vapor molecules onto the glass-fiber surfaces at locations within the insulation where the relative humidity is below 100%. Condensation (or ablimation‡ of frost where the local temperature is below the freezing point) occurs at locations where the local relative humidity is at 100%. Since water vapor adsorption is usually less than the mass of condensation, the amount of moisture which accumulates within the insulation is usually greater in regions where condensation takes place. Moisture accumulation due to adsorption occurs at the molecular level; i.e. mono-layers of water vapor molecules collect on the surfaces of the glass-fibers [6].

Condensation phenomenon has been observed in porous wall insulation, particularly when the material is exposed to a high relative humidity with large temperature differences [7]. As condensation occurs, the latent heat of condensation (or ablimation) is released, acting as a heat source in the heat transfer process. Energy is also released during the adsorption process as the molecules of water vapor become attached to the glass-fiber surfaces. Although the amount of moisture accumulation through adsorption is usually much smaller than that for condensation, the heat of adsorption can be up to four times as high as the heat of vaporization. Also, experimental evidence shows that the thermal energy exchange between the

† Author to whom correspondence should be addressed. Current address: Department of Mechanical Engineering, Tennessee State University, Nashville, TN 37209, U.S.A.

‡ Ablimation means a substance changing from its vapor phase to a solid phase [15]; here, it means frost accumulation from water vapor.

NOMENCLATURE

T_c	cold plate temperature	W	humidity ratio.
T_∞	inlet air temperature		
ΔT	temperature difference		
u_g	air velocity	Greek symbol	
$\dot{V}$	inlet air flow rate	ϕ_∞	inlet air relative humidity (RH).

adsorbed phase and the surrounding phases during an adsorption or desorption process is pronounced and can alter the local temperatures significantly [6, 8].

It has been found that the main reason for moisture accumulation within building wall cavities is the exfiltration of warm, humid, indoor air during the heating season [9]. Vafai and Tien [10] found, from their numerical simulation for test conditions applied to a warm humid climate, that air movement within the porous insulation is often the dominant mode of energy and mass transfer. This applies even for very small pressure gradients across the slab. This would indicate that, in studying the moisture accumulation and heat transfer processes within building wall insulation materials, attention should be placed on the temperature and humidity properties of airflow through the insulation, as well as the flow direction. This is particularly important for cold weather applications. It has been reported that frosting, coupled with condensation and adsorption, has a more significant effect on the thermal performance of fiberglass insulation than that in warm climate applications [8, 13, 14]. To the authors' knowledge, there have been very few if any experimental results for laboratory tests that quantify the effect of air movement on moisture and frost accumulation for cold climate applications. The experimental validation of numerical models is even more scarce.

In order to fully understand the phenomena occurring within the wall structure, research needs to be conducted into the effects of both air exfiltration (which results in the accumulation of moisture and frost within the porous insulation inside wall cavities), and air infiltration (which may tend to remove moisture/frost from some regions of an insulation slab and deposit this moisture as condensation or frost elsewhere). It is the objective of this investigation to examine experimentally the effects of air exfiltration and air infiltration on the heat and moisture transfer characteristics of a medium density porous fiberglass insulation.

2. EXPERIMENTAL SCHEME

The overall experimental requirement was to create a uniform, one-dimensional flow of air through a porous fiberglass insulation slab. The airflow was to simulate exfiltration and infiltration conditions through a house wall or ceiling during cold weather (e.g. internal environment—moist air at $+20^\circ C$, external environment—dry air at $-20^\circ C$). Although typical indoor relative humidity conditions during cold winter weather rarely exceed 50% relative humidity (RH) in most buildings, the exfiltration tests were conducted with warm, room temperature air with a high relative humidity (60–90% RH). These high relative humidities were used in order to obtain experimental data with small relative errors and to magnify the effects that varying the relative humidity might have on the heat, moisture and air transport characteristics within the porous insulation slab. It should be noted, however, that for certain buildings and rooms (some houses, animal barns, indoor swimming pools, hospital operating rooms, computer rooms, etc.) the internal relative humidity can reach 50% or higher during cold weather.

A schematic drawing of the experiment test section is provided in Fig. 1. The test insulation slab is placed horizontally and cooled from below. This configuration allows us to exclude buoyancy flow from the model. For the air exfiltration tests warm air was supplied to the air inlet ports at the top of the test cell (eight are provided in the top cover plate) and flowed uniformly down toward the cold plate on the bottom. For the air infiltration tests cold air was supplied to the air gap through eight other inlet ports located in the bottom air gap region and the air flowed uniformly up toward the top cover plate, which was at room temperature.

A four-layer, medium-density (50 kg m^{-3}), glass-fiber slab (AF 545 Fiberglas Canada, ON) with a total dimension of $275 \times 600 \times 90$ mm was placed in the test section for each test. A cold plate, which could be cooled to well below the triple-point temperature of water through a heat exchanger, was located at the bottom of the test section. By placing nine small plastic disc spacers on top of the cold plate, an air gap was created between the bottom surface of the insulation slab and the cold plate (approx. 12 mm in height). This permitted the exfiltration or infiltration air to flow uniformly through the insulation slab. To start a test, the volumetric airflow rate was set using a mass flow controller, and the ethylene glycol–water solution, which was used as the heat exchanger coolant for the cold plate, was pumped from a storage tank which was placed in an environmental chamber.

Ten thermocouples (accuracy ± 0.2 K) were placed between the glass fiber layers and on the exposed

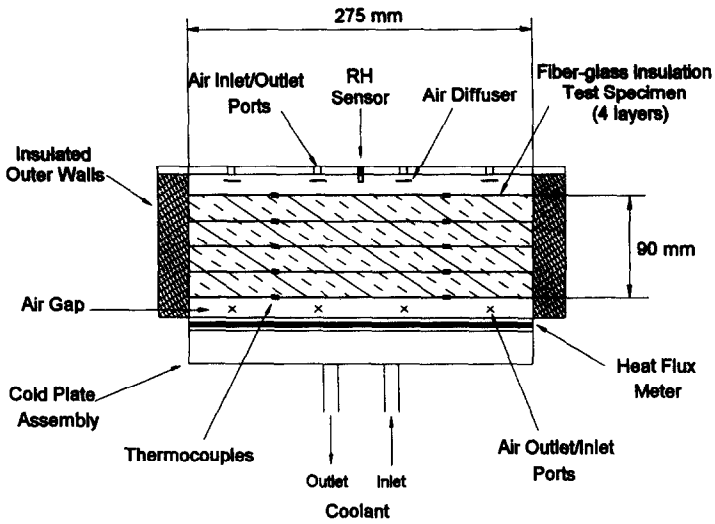

Fig. 1. Schematic drawing of experiment test section.

top and bottom surfaces of the slab to measure the temperature field throughout the slab. The moisture accumulation in each layer of insulation at the end of each test was determined by weighing the layers prior to (dry) and at the end of each experiment (moisture accumulation uncertainty $\pm 5\%$ to $\pm 15\%$ depending on samples). To ensure consistent 'dry' results, each testing sample was initially conditioned by the same procedure; i.e. 16 h oven dry at 107°C and 4 h natural convection cooling to room temperature. A calibrated humidity sensor (uncertainty $\pm 2\%$ RH) was placed in the top cover plate of the experimental test section. This sensor was used to ensure that the air entering the insulation slab for the exfiltration tests had the correct relative humidity, whereas, for the infiltration tests, it was used to monitor the outlet air relative humidity. To measure the temperature of the air leaving the air gap at the bottom of the test sample, a single thermocouple was placed at the center of the plate in the middle of the air gap between the insulation and the cold plate.

A heat-flux meter was mounted within the cold plate to measure the heat flux through the cold plate. As illustrated in Fig. 2, the heat-flux meter consisted of a high thermal resistance polyethylene sheet (thermal conductivity of 0.2177 W m^{-1} K^{-1}, as given by the manufacturer) with a thickness of 1/8 in. (3.175 mm). An aluminum test plate with a thickness of 1/8 in. was mounted on top of the polyethylene sheet to keep the top surface temperature uniform. Twenty-one pairs

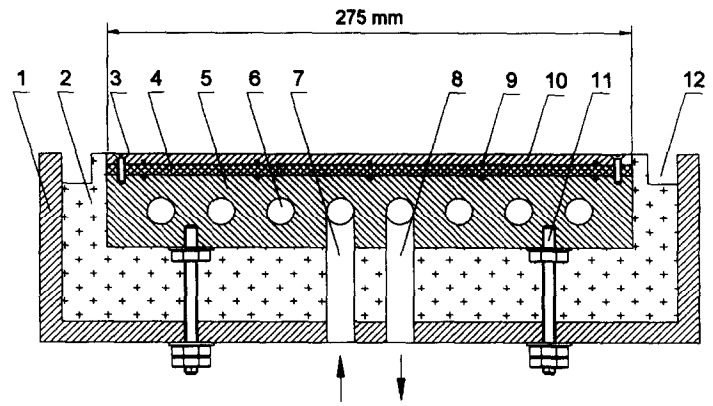

Fig. 2. Heat-flux meter and cold plate assembly.

of thermocouples were embedded in the lower and upper aluminum surfaces on either side of the polyethylene sheet. The gaps between the polyethylene sheet and the top aluminum plate, and the polyethylene sheet and the cold block, were filled with a very thin layer of thermal paste to minimize the contact resistance between these surfaces (thermal compound, part no. 120-8 with a thermal resistance of 0.06 K m^2 W^{-1}). The thermal conductance (W m^{-2} K^{-1}) of the heat-flux meter was calibrated based on the measured temperature drop across a thermally aged 1 in.-thick sheet of extruded Styrofoam, which was placed on top of the cold plate assembly.

For each experiment, a number of measurements were recorded in order to determine temperature profiles, heat flux and moisture accumulation values. These measurements included temperatures within and across the insulation slab and within the air gap between the insulation and the cold surface, frost/moisture accumulation measurements within the insulation and on the surface of the cold plate, air flow rates, and the relative humidity of the supply air (for the exfiltration case) and the exhaust air (for the infiltration case).

The range of air flow velocity used in this study was established based on a field investigation by Shaw [11]. This investigation found that a typical detached Canadian residential house experiences an air exfiltration rate of 0.98 l m^{-2} s^{-1}. For a typical house size this means an average air speed through the building envelope filled with insulation of about 1.0 mm s^{-1}. According to Ogniewicz and Tien [12], air velocities encountered in typical porous insulation applications, due to free convection and air infiltration, are also of the order of 1.0 mm s^{-1}. In this study, tests were carried out with the average air flow velocity through the insulation at 0.5, 1.0 and 1.5 mm s^{-1}.

3. EXPERIMENT APPARATUS

Figure 3 outlines the assembly of the components used for the exfiltration experiments, where warm moist air flowed into the top of the test cell, shown in Fig. 1, and uniformly flowed down toward the cold plate at the bottom. Compressed air first passed through an industrial dryer, which removed most of the unwanted moisture from the supply air, and then flowed through the mass flow controller at the desired airflow rate. In generating the required range of inlet air relative humidity (60–90% RH), a water bath was implemented. By regulating the flow using a flow meter and a control valve, a portion of the dry inlet air was diverted from the main line to the bottom of the water bath. As the air moved up through the bath it became saturated (100% RH). By mixing this saturated air with dry air in the correct proportions, the desired air relative humidity was attained. Once the proper relative humidity had been obtained, the air was directed into the top portion of the test section through eight inlet ports. A total of 16 tests were performed to study the effects of air exfiltration on the processes occurring within the porous insulation. The initial set of tests was performed for all three inlet air relative humidity values (60, 75, 90%) for test durations of 1, 2 and 3 h with the airflow rate at 10 l min^{-1}, which resulted in an average air velocity within the insulation of 1.0 mm s^{-1}. It was discovered from the measured data that the temperature profiles throughout the insulation slab reached a quasi-steady state after a period of only 2 h. Therefore, for the 15 l min^{-1} air flow rate (i.e. 1.5 mm s^{-1} air speed within the insulation), only 1 and 2 h experiments were performed for each of the three inlet air relative humidity values. To obtain a more complete data set showing the effect that varying the airflow rate through the

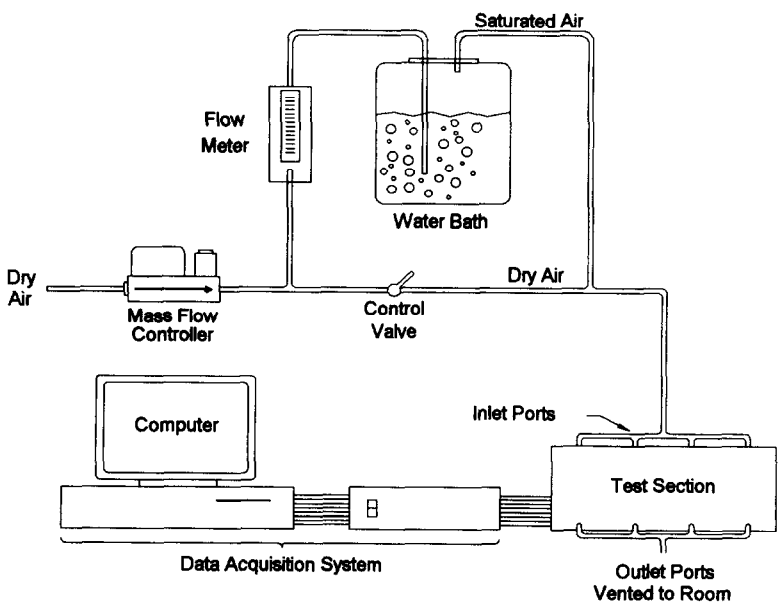

Fig. 3. Exfiltration apparatus.

Table 1. Experimental conditions for air exfiltration

Property	Value	Test variation
T_∞ (inlet air temperature)	20.0°C	±1.0°C
T_c (cold plate temperature)	−20.0°C	±1.0°C
ϕ_∞ (inlet air RH)	60% 75% 90%	±2.0%
$\dot{V}$ (inlet airflow rate)	8.33×10^{-5} m^3 s^{-1} (5 l min^{-1}) 1.67×10^{-4} m^3 s^{-1} (10 l min^{-1}) 2.50×10^{-4} m^3 s^{-1} (15 l min^{-1})	±1.0%

insulation might have on the transport properties, a 2 h test was performed at 5 l min^{-1} (i.e. 0.5 mm s^{-1} air speed within the insulation) with the inlet air relative humidity at 75%. At the end of each of these tests, the frost and moisture mass accumulation data were obtained. Table 1 lists the range of parameters used in the air exfiltration study.

Figure 4 outlines the assembly of the components required to carry out the air infiltration experiments where cold air entered the air gap and uniformly flowed up through the insulation to the top of the test cell in Fig. 1. The infiltration tests involved passing cold dry air through the porous media from the cold side of the slab towards the warm side. In the case of air infiltration, the drying process of the inlet supply air took place in two stages. The air from the compressor passed through an industrial drying machine and then it passed through a desiccant to eliminate even more of the moisture which might be present in the airflow, before it was cooled to the cold plate temperature. Each of the five tests which involved air infiltration consisted of first 2 h of air exfiltration (so that there would be moisture distributed throughout the insulation sample at the start of the infiltration tests), immediately followed by 2 h of air infiltration. The infiltration air supplied to the test cell was dry (i.e. humidity ratio, $W = 0.0008$), therefore little would have been observed if the insulation sample had also been dry at the start of the infiltration tests. Since the experimental moisture/frost accumulation data had already been obtained for the exfiltration tests, the starting conditions for the infiltration portion of these tests were known. By using these known data and those obtained at the end of the infiltration tests, the effect of air infiltration on the moisture transport properties within the insulation was determined. For each complete 4 h test, the airflow rate was kept constant, although the direction of the flow was reversed after 2 h. Furthermore, the temperature and relative humidity of the infiltration air were kept the same for all of the tests performed (dry air, −20°C). For the exfiltration portion of these tests, the inlet air RH was kept at 75% for both the 0.5 mm s^{-1} and 1.5 mm s^{-1} air velocities, whereas for the 1.0 mm s^{-1} flow rate tests were carried out with the inlet air RH at 60, 75 and 90%. Changing the airflow rate and the relative humidity of the inlet air for the exfiltration portion resulted in different initial conditions (temperature profiles and moisture accumulation) for the air infiltration tests.

To cool the supply air, Tygon tubing was wrapped around the supply line which carried the ethylene glycol–water solution used to cool the cold plate, and insulation was then placed over top of these wrappings. The dry air was passed through this tubing and up to the test cell. With the supply piping at approx.

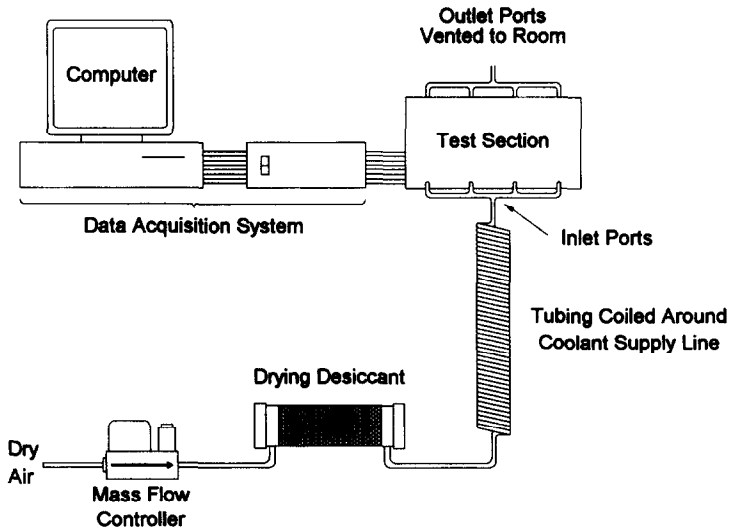

Fig. 4. Infiltration apparatus.

Table 2. Experimental condition for air infiltration

Property	Value	Test variation
T_∞ (inlet air temperature)	-20.0°C	± 1.0°C
T_c (cold plate temperature)	-20.0°C	± 1.0°C
ϕ_∞ (inlet air RH)	$\approx 5\%$	$\pm 2\%$ RH
$\dot{V}$ (air flow rate)	5 l min^{-1} ($u_g = 0.5$ mm s^{-1}) 10 l min^{-1} ($u_g = 1.0$ mm s^{-1}) 15 l min^{-1} ($u_g = 1.5$ mm s^{-1})	$\pm 0.80\%$

-24°C, and the total number of tubing wrappings near 200, the air was cooled to the required temperature of -20°C. Table 2 lists the parameter settings for the infiltration tests.

4. EXPERIMENTAL RESULTS

4.1. *Air exfiltration*

Figure 5 represents a typical temperature profile for a 3 h exfiltration test. The symbols used in the figures and tables are noted as follows: L = total thickness of the insulation slab [m]; z = coordinate axis with $z = 0$ at the warm side and $z = L$ at the cold side of the slab [m]; T = temperature [K]. The temperatures in the upper region of the slab, particularly in the initial transient period, where the temperatures rose above the ambient temperature, were above the saturation temperature based on the vapor density of the inlet air. This indicated that condensation could not have been occurring in this region. Therefore, the energy required for the temperature increase resulted from adsorption. On a molecular level, as the water vapor passed through the glass-fiber porous media, adsorption of water molecules from the water vapor onto the glass-fiber surfaces was taking place. This phenomenon is similar to the test results obtained under no exfiltration (vapor diffusion only), as reported by Tao *et al.* [8]. Since the slab was initially dry, the sudden exposure of the insulation to moist airflow resulted in a phase change energy release due to the adhesion of the water molecules to the fiber surfaces. As indicated in this figure, the temperatures throughout the insulation slab and that within the air gap between the slab and the cold plate reached a steady state (all of which are below the ambient temperature) after a period of approx. 2 h.

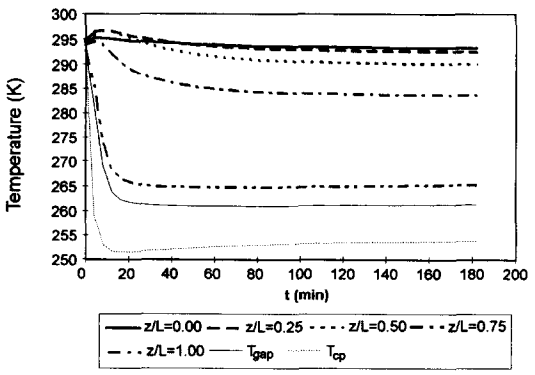

Fig. 5. Typical temperature profiles for an air exfiltration test (10 l min^{-1}, 75% RH).

The release of energy, which resulted in the temperature increase, is referred to as the heat of adsorption (which can be up to four times higher than the heat of evaporation or condensation [6]). The temperatures continued to increase only as long as the energy released during this adsorption process was dominant compared to the heat diffusion toward the cold temperatures created by the cold plate below the insulation slab. It should be noted that, after a short period of time (when the moisture content reached 0.05% of the dry mass of the insulation), the heat of adsorption equaled the heat of condensation and they remained the same as long as the moisture content stayed above this particular level [6].

Under air exfiltration conditions, adsorption strongly affected the temperatures in the middle of the slab. However, for the vapor-diffusion-only process, under similar temperature and air relative humidity boundary conditions, the temperature rise due to the adsorption effect was only detected at locations near the top surface of the slab [8]. This difference occurred because, in the exfiltration tests, as a result of the downward movement of air through the insulation slab, the adsorption process took place in a larger domain as compared with the process with only vapor diffusion. Correspondingly, the domain in which the temperatures increase above the ambient temperature became larger as well.

Table 3 lists the temperature increases (ΔT) due to adsorption (maximum temperature $-$ initial temperature) at the locations of $z/L = 0.0$, $z/L = 0.25$, $z/L = 0.50$ and $z/L = 0.75$ for all of the exfiltration experiments. This table indicates that an increase in the inlet air relative humidity (maintaining a constant airflow rate) resulted in larger temperature increases at all four locations. As the inlet air RH increased, the number of water vapor molecules in the air available for adsorption to the fiber surfaces increased. Therefore, since the amount of adsorption taking place increased, the energy released was higher, thus resulting in larger temperature increases. Table 3 also shows that increasing the airflow rate (at constant inlet air relative humidities) shifts the point of maximum temperature increase due to adsorption closer to the cold surface. In examining the 75% inlet air relative humidity case, the maximum temperature increase

Table 3. Maximum temperature increases in the fiberglass associated with adsorption

Flow rate [l min^{-1}]	Relative humidity [%]	ΔT $z/L = 0.00$	ΔT $z/L = 0.25$	ΔT $z/L = 0.50$	ΔT $z/L = 0.75$
5	75	+1.19	+1.94	+1.53	+0.00
10	60	+0.66	+1.70	+2.08	+0.60
	75	+0.83	+1.99	+2.27	+0.74
	90	+1.05	+2.61	+2.85	+1.02
15	60	+0.36	+1.55	+2.10	+1.32
	75	+0.66	+2.10	+2.99	+1.92
	90	+0.74	+2.79	+3.64	+2.69

shifted from the $z/L = 0.25$ location for the 5 l min^{-1} test to the $z/L = 0.50$ location for the 15 l min^{-1} test. It should also be noted, however, that, while this shift was taking place, the temperature increase due to adsorption in the upper layers of insulation decreased. As the water vapor passed through the slab at a higher velocity (higher airflow rate), the adsorption temperature increase, ΔT, in the upper layers of the insulation was reduced by the convective heat transfer due to the airflow, which was supplied at a cooler temperature at the top of the insulation.

Increasing the inlet air relative humidity (Fig. 6), or increasing the airflow rate (Fig. 7), both resulted in a substantial increase in the total amount of moisture/frost which accumulated within the bottom layer of the insulation slab. Each data point represents a ratio of the mass of accumulated moisture within each insulation layer divided by the dry mass of each layer. Within the upper three layers of the slab, increasing the inlet air RH or increasing the airflow rate had very little effect on the degree of moisture accumulation. In comparing the two figures, it is evident that increasing the rate of air flow through the insulation had a greater effect on the moisture accumulation near the cold surface than increasing the relative humidity of the inlet air (e.g. increasing the flow rate from 5 to 10 l min^{-1} increased the moisture accumulation by 150% in the bottom layer, whereas increasing the relative humidity from 60 to 90% increased the moisture accumulation by only 85%).

As indicated in Figs. 6 and 7, the majority of the moisture was collected in the layer closest to the cold surface. This observation is the same for all of the tests carried out in the exfiltration study. With the temperatures within the bottom layer dropping below the saturation temperature, based on the vapor density at such locations, condensation/ablimation took place. Although moisture accumulation took place within the upper regions of the slab due to adsorption, the amount of moisture which accumulated was much less than that for the condensation region, since adsorption deals with the deposition of moisture onto the fiber surfaces in much smaller molecular layers.

This trend of having the maximum amount of moisture accumulation near the cold surface is similar to the test results obtained with no exfiltration (vapor diffusion only [13]), but contrary to the numerical results presented by Vafai and Tien [10]. This may be due to the fact that the time duration for moisture accumulation in Vafai and Tien's numerical results was much shorter than for the tests presented here. In the study by Tao *et al.* [14], it was also found that, during the initial period, more moisture accumulated near the warm side of the insulation slab, while later more moisture and/or frost was found near the cold side of the slab. It should be noted that for operating temperatures above the freezing point, moisture accumulation is not significant even with air infiltration/exfiltration; e.g. Vafai and Tien [10] reported a liquid volume fraction of the order of 10^{-4} with the operating temperatures above the freezing point. With frosting, however, the moisture accumulation in the

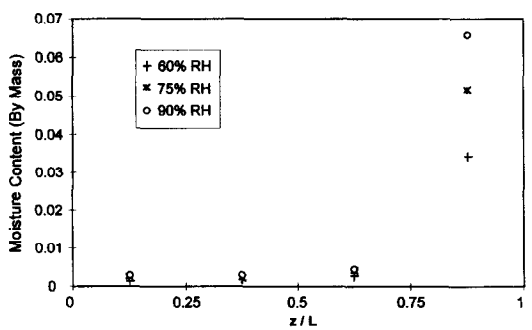

Fig. 6. Moisture accumulation profiles for a range of relative humidities (10 l min^{-1}, after 2 h).

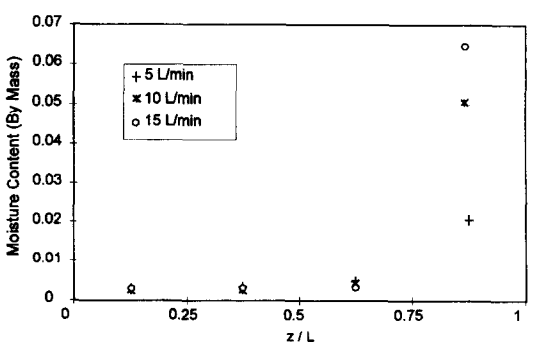

Fig. 7. Effect of air flow rate on moisture accumulation (75% RH, after 2 h).

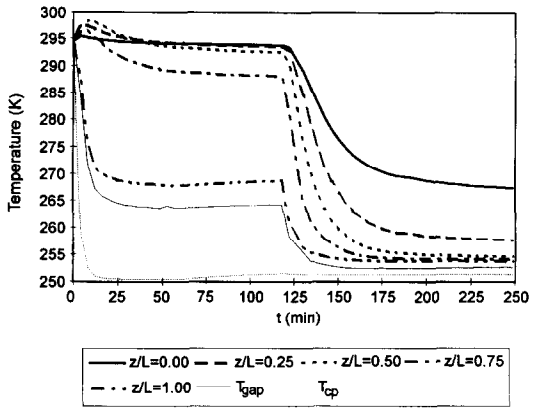

Fig. 8. Temperature profiles throughout the slab for air exfiltration (0–120 min, 75% RH, 10 l min^{-1}) and air infiltration (120–240 min, 10 l min^{-1}).

bottom slab was more pronounced during warm air exfiltration; i.e. the moisture content reached 0.09 by mass or about 4.5×10^{-3} liquid volume fraction for the 90% RH, 10 l min^{-1} case ($u_g = 1.0$ mm s^{-1}), which is a factor of 45 greater than the case without frost [10].

4.2. *Air infiltration*

Figure 8 depicts the temperature profiles of a complete 4 h test for exfiltration and infiltration. By the end of the first 2 h (exfiltration), the temperature profile within the insulation slab is shown to reach steady state. At this time the airflow system was reconfigured (in less than 2 min) from Fig. 3 to Fig. 4 for air infiltration. The temperatures within the insulation rapidly decreased until, eventually for this test, the temperatures at $z/L = 0.50$, $z/L = 0.75$, and $z/L = 1.00$ became within 1°C of each other.

Figure 9 compares the experimentally determined amount of moisture/frost accumulation within the insulation slab after a 2 h exfiltration test (10 l min^{-1}, $u_g = 1.0$ mm s^{-1}, 75% inlet air RH) to the amount present after an additional 2 h of air infiltration (10 l min^{-1}, $u_g = 1.0$ mm s^{-1}). This figure indicates that, during the infiltration process, the dry inlet air was sublimating frost from the bottom layer of insulation, and as the air passed through the upper layers, some of the water vapor was being re-deposited, either through ablimation or condensation. The net effect was that the total mass of frost and condensate was reduced by air infiltration through the slab of insulation.

In comparing the experimental moisture accumulation results obtained for the various airflow rates, a significant phenomenon was observed. Based on the total amount of moisture contained within the entire insulation slab after the exfiltration and infiltration tests (kg moisture/kg dry insulation material) as the airflow rate was reduced, a significant percentage of the moisture accumulated after air exfiltration was removed from the slab during air infiltration. Figure 10 compares the air infiltration moisture (or frost) removal mass as a fraction of the accumulated moisture (or frost) at the end of the air exfiltration period for the three airflow rates. This figure clearly shows that a higher drying rate was achieved by lowering the rate of air flow during air infiltration.

Increasing the infiltration airflow rate caused the temperatures to decrease throughout the slab, thus shifting the boundary or interface between the wet and frozen regions up towards the top surface of the insulation slab. Any moisture below this interface existed as frost and could only be removed or deposited by sublimation or ablimation, whereas any moisture above this interface could be removed or deposited by evaporation or condensation (which occur at a higher rate than sublimation or ablimation). For air infiltration and the lowest airflow rate (5 l min^{-1}), the point at which moisture froze was the closest to the bottom surface of the slab. When the flow direction was switched for infiltration, the 0°C interface moved up towards the top surface at the slowest rate, as compared to the results obtained from the other airflow rates. Therefore, more of the accumulated moisture within the slab was in liquid form for a longer period of time, and thus more evaporation could take place. Another very important factor in the removal of moisture or frost from the insulation is the ambient air temperature and saturation humidity ratio. The higher the air temperature the larger the humidity ratio at saturation conditions.

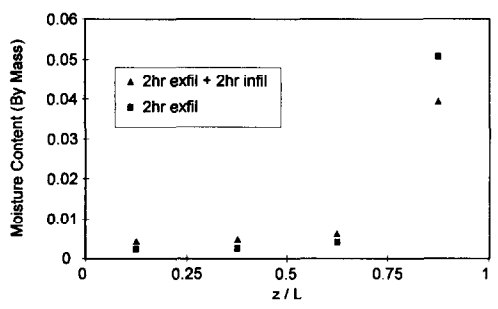

Fig. 9. Moisture accumulation comparison—exfiltration/infiltration (10 l min^{-1}, 75% RH exfiltration air).

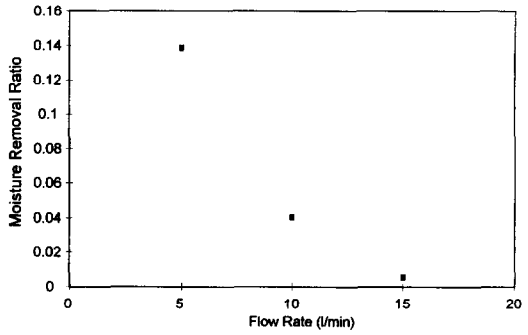

Fig. 10. Moisture removal ratio for various airflow rates.

4.3. *Heat flux at the cold plate*

The current design of the experimental apparatus allows us to measure directly the heat flux at the cold plate during each test (Fig. 2). It is, however, of greater interest for us to quantify the heat flux through fiberglass insulation. In principle, this heat flux can be derived from an energy balance approach considering air gap temperature, frost accumulation on the cold plate surface and measured heat flux at the cold plate. Such an attempt did not lead to a convincing accuracy, due to various limitations in measurement technique, including the large uncertainty in determining the energy term associated with frost accumulation [16]. Since this methodology has considerable future merit and it is discussed further in the companion paper [17], we report the status of the experimental technique and provide numerical analysis of heat flux through thermal insulation under air filtration conditions. The numerical results, verified by the experimental data of temperature and moisture content [17], could be used as a guide to evaluate the thermal and mass transfer performance.

5. SUMMARY AND CONCLUSIONS

To date, there has been no laboratory research reported to investigate the effects of air flow through a porous fiberglass insulation material (either exfiltration or infiltration), while the material is subjected to sub-zero temperatures. There has been no quantitative information which examines the effects of varying such parameters as the inlet air relative humidity, inlet airflow rate, or duration of the exposure on the heat and mass transfer processes taking place within the insulating material.

This work was aimed at measuring the processes taking place within the fiberglass insulation with frosting effects and showing the effects that airflow through the wall insulation can have on the heat loss to the exterior of a building. The physical importance of reducing or eliminating any air flow through insulated structures with the use of a properly installed vapor retarder has been made clear.

The results obtained through this research work lead to the following conclusions:

Air exfiltration

(1) The adsorption process significantly increased the initial temperatures within the top portion of the slab (up to 3.6°C for the tests carried out here). Furthermore, increasing the airflow rate from 5 to 15 l min^{-1} (u_g = 0.5–1.5 mm s^{-1}) shifted the region of maximum temperature increase due to adsorption from $z/L = 0.25$ to $z/L = 0.50$ (farther into the slab—closer to the cold region).

(2) The majority of the moisture and frost accumulated within the bottom layer of the insulation slab. Furthermore, increasing the inlet air relative humidity from 60 to 90% resulted in an 85% increase in the moisture accumulation in the bottom layer, while increasing the airflow rate from 5 to 10 l min^{-1} increased the moisture accumulation in the bottom layer by 150%.

Air infiltration

(1) An airflow rate of 5 l min^{-1} (u_g = 0.5 mm s^{-1}) produced a drying rate which was 26 times greater than that for an airflow rate of 15 l min^{-1} (u_g = 0.5 mm s^{-1}); i.e. the lower the air flow rate through the insulation, the higher the drying rate. Lower airflow rates produced warmer temperatures throughout the slab, with a larger amount of the moisture within the slab existing in the liquid state as opposed to frost (more of the slab was above 273 K).

REFERENCES

1. C. P. Hedlin, Effect of moisture on thermal resistances of some insulations in a flat roof system under field-type conditions, ASTM STP 789, pp. 602–625 (1983).
2. J. Lstiburek and J. Carmody, *Moisture Control Handbook*. Oak Ridge National Laboratory, ORNL/Sub/89-SD 350/1 (1990).
3. NBC, *National Building Code of Canada*. National Research Council, Canada (1990).
4. M. K. Kumaran, Moisture transport through glass-fiber insulation in the presence of a thermal gradient, *J. Thermal Insul.* **10**, 243–255 (1987).
5. ASTM, *Water in Exterior Building Walls: Problems and Solutions* (Edited by T. A. Schwartz). ASTM STP 1107, Philadelphia, PA (1991).
6. Y.-X. Tao, R. W. Besant and C. J. Simonson, Measurement of the heat of adsorption for a typical fibrous insulation, *ASHRAE Trans.* **98**(2), 495–501 (1993).
7. K. Vafai and H. C. Tien, A numerical investigation of phase change effects in porous materials, *Int. J. Heat Mass Transfer* **32**, 1261–1277 (1989).
8. Y.-X. Tao, R. W. Besant and K. S. Rezkallah, The transient thermal response of a glass-fiber insulation slab with hygroscopicity effects, *Int. J. Heat Mass Transfer* **35**, 1155–1167 (1992).
9. M. K. Kumaran, Heat, air and moisture transport through building materials and components: can we calculate and predict?, *Proceedings of the Sixth Conference on Building Science and Technology*, pp. 129–144, University of Waterloo (1992).
10. K. Vafai and H. C. Tien, A synthesis of infiltration effects on an insulation matrix, *Int. J. Heat Mass Transfer* **33**, 1263–1280 (1990).
11. C. Y. Shaw, Methods for estimating air exchange rates and sizing mechanical ventilation systems for houses, *ASHRAE Trans.* **93**, 2284–2302 (1987).
12. Y. Ogniewicz and C. L. Tien, Analysis of condensation in porous insulation, *Int. J. Heat Mass Transfer* **24**, 421–429 (1981).
13. Y.-X. Tao, R. W. Besant and K. S. Rezkallah, Unsteady heat and mass transfer with phase changes in an insulation slab: frosting effects, *Int. J. Heat Mass Transfer* **34**, 1593–1603 (1991).
14. Y.-X. Tao, R. W. Besant and K. S. Rezkallah, Heat and moisture transport through a glass-fiber slab with one side subjected to a freezing temperature. In *Water in Exterior Walls: Problems and Solutions*, ASTM STP 1107, pp. 92–104 (1991).

15. A. V. Luikov, *Heat and Mass Transfer in Capillary-porous Bodies* (Translated by P. W. B. Harrison and Translation Edited by W. M. Pun), p. 254. Pergamon Press, Oxford (1966).
16. D. R. Mitchell, The effects of air exfiltration/infiltration on the transient thermal response of a glassfiber insulation slab, M.Sc. Thesis, University of Saskatchewan (1994).
17. D. R. Mitchell, Y.-X. Tao and R. W. Besant, Air filtration with moisture and frosting phase changes in fiberglass insulation—II. Model validation, *Int. J. Heat Mass Transfer* **38,** 1597–1604 (1995).